CONF-891007--30

DE90 001972

TECHNOLOGY OF FAST-WAVE CURRENT DRIVE ANTENNAS*

D. J. Hoffman, F. W. Baity, R. H. Goulding, G. R. Haste, P. M. Ryan, D. J. Taylor, D. W. Swain, M. J. Mayberry,† and J. J. Yugo

Oak Ridge National Laboratory, P. O. Box 2009, Oak Ridge, TN 37831-8071

ABSTRACT

The design of fast-wave current drive (FWCD) antennas combines the usual antenna considerations (e.g., the plasma/antenna interface, disruptions, high currents and voltages, and thermal loads) with new requirements for spectral shaping and phase control. The internal configuration of the antenna array has a profound effect on the spectrum and the ability to control phasing. This paper elaborates on these considerations, as epitomized by a proof-of-principle (POP) experiment designed for the DIII-D tokamak. The extension of FWCD for machines such as the International Thermonuclear Engineering Reactor (ITER) will require combining ideas implemented in the POP experiment with reactor-relevant antenna concepts, such as the folded waveguide.

INTRODUCTION

The long-term engineering requirements for fusion reactors include the development of a noninductive means to drive current in the plasma because of the need for steady-state operation. The ITER design calls for 115 MW of power to generate 18 MA of plasma current for pulse lengths of >120 s.[1] Negative ion beams and lower hybrid waves are being considered for this function. Both techniques have serious limitations. Experiments on Alcator-C, PLT, and JT-60 have shown that lower hybrid current drive faces an effective plasma density limit that is below the desired operating density of ITER. The negative ion beams face a different type of problem: they require large amounts of space near the machine, and they are extremely expensive to manufacture and develop (historically, beams have cost roughly two to four times as much as ion cyclotron heating). Nonetheless, the negative ions are perceived as the choice for current drive on ITER because there is some proof that beams can drive currents.

The cost of beams is so high and the risk of high-energy operation is so great that there is some impetus to develop an alternative method of current drive. Recent analyses by Ehst,[2] Batchelor,[3] and Mau[4] have shown that ion cyclotron waves could be used to drive the currents. The predicted efficiencies for FWCD in ITER are virtually the same as those for negative ion beams. The FWCD looks especially attractive because the equipment is compact and the power is inexpensive and easily transported. However, FWCD suffers from the lack of any experimental verification. Thus, a POP experiment was designed for the DIII-D experiment to confirm that FWCD works and is efficient.

The physics analyses are based on asymmetrically modifying the electron velocity distribution with a nonresonant, traveling ion cyclotron wave. The electrons must be be warm enough to absorb the power by either Landau damping or transit-time magnetic pumping (TTMP). These physical mechanisms translate into technology requirements in the following manner. The antenna should be a phased array with arbitrary phasing to generate the traveling wave. The majority of the wave power needs to be in the low spectral range ($n_{\parallel} \approx 2$–5) with directivity so that the interaction with electrons results primarily in net electron current and not heating. During the current drive, the collisionality must be low so that energy is not dumped into the bulk of the velocity distribution. This generally means that densities will be low, and so will the rf loading. The FWCD frequency is in the range from 20 to 120 MHz for ITER. The net result of all these considerations is that FWCD should be possible with an array of rf antennas that face the standard tokamak conditions, under the additional constraints of phase control and spectral content centered at low wave numbers for current drive with little content at higher wave numbers (which result only in heating).

THE DIII-D PROOF-OF-PRINCIPLE DESIGN

A POP experiment[5,6] has been devised for the DIII-D tokamak to demonstrate FWCD on a large tokamak. The target plasma parameters are $B \approx 1$ T, $n \approx 1.3 \times 10^{13}$ cm^{-3}, $T_e \approx 4$ keV, and $I_p \approx 0.5$ MA. The expected plasma current resulting from ≈2 MW of coupled rf power for 1 s is predicted to be ≈0.25–0.5 MA, which is a significant fraction of the total ohmic current. The antenna is a 50- by 100-cm, four-strap array that fits into a vacuum wall recess, as shown in Fig. 1. The antenna is designed for

*Research sponsored by the Office of Fusion Energy, U.S. Department of Energy, under contract DE-AC05-84OR21400 with Martin Marietta Energy Systems, Inc.

†General Atomics, San Diego, California 92138.

operation at 30–60 MHz, with arbitrary phasing.

The mechanical design parameters fall into the usual two categories—disruption forces and thermal stresses. Since the design has four loops, with the attendant coaxial transmission lines linking the antenna boxes with the port, disruption torques (<125,000 in.•lb) for the array are considerably greater than those on a single loop. Thermal loads are not significantly different from those on a single antenna. The design plasma loads were 50 W/cm^2 radially, and the rf loads were 40 W/cm^2 with a peaking factor of 4.

The task of obtaining the desired spectrum is more difficult than with antennas for ICRF heating because of the directionality requirement. Measurements on a quarter-scale and a full-scale mock-up of the DIII-D antenna demonstrate the problem (Fig. 2). In two cases—one with a dividing wall or septum between straps and one without—the antenna straps were phased at 90° between straps. The solid septa resulted in a large fraction of power in the anticurrent direction centered around $n_{||} \approx -20$ and the desired peak around $n_{||} \approx 7$. The spectrum for the case without septa shows a small amount of power in the $n_{||} = -20$ peak. Two questions arise: what happens to the power in these undesired peaks, and can power in the undesired peaks be avoided?

The question of what happens to the power in these peaks is unresolved. These peaks correspond to power going into direct heating of the electrons. This is not necessarily bad, but it may obfuscate the experiment. The second concern about this peak is that the plasma response may be lower because of inherently greater edge attenuation or lower plasma surface impedance. Given the overall uncertainty about the plasma response to high wave numbers, it is desirable to avoid this part of the spectrum.

The question of avoiding the undesired peaks would seem to have an obvious answer, as shown in Fig. 2—run the antenna with the good spectrum. The antenna array comprises four antennas, each with its own spectrum F(k). With adjacent straps having merely a spatial and phase displacement, the total spectrum, G, is

$$G(k) = F(k) \cdot A(k), \quad A(k) = \Sigma \exp(ikx_n - \phi_n) \ , \qquad (1)$$

where A is the array factor, x_n is the spatial displacement of the nth antenna, and ϕ_n is the relative phase of the nth strap. Figure 3 shows the array factors for a 4-strap and a 12-strap array. Clearly, the array factor increases the spectral power in the desired region and suppresses the power away from it. The higher the number of straps, the better the suppression of undesired peaks. However, the periodicity of the array factor (proportional to the inverse of the spatial displacement) means that some peaks cannot be suppressed. In the typical single antenna spectrum, most of the power is in wave numbers corresponding to the current strap and the cavity widths (typically, $n_{||} = \pm 10 - 30$). A small amount of power is in the $n_{||} \approx 5$ range, which is then amplified by the array factor. However, if there is substantial power in the negative peak and if it coincides with the array peak, the spectrum becomes unoptimized. Clearly, the goal is then to tailor the single antenna spectrum. The negative currents in the solid sidewalls serve to minimize the low-wave-number power relative to the high-wave-number power. Slotted or no-septum arrays move the return current away from the interaction zone of the antenna, thereby maximizing the low-wave-number power.

The control of the antenna array and its spectrum is complicated by the mutual coupling between straps. This can be illustrated by considering two coupled straps with voltages

$$V_1 = (j\omega L + R) \cdot I_1 + j\omega KL I_2 \ , \qquad (2)$$
$$V_2 = (j\omega L + R) \cdot I_2 + j\omega KL I_1 \ , \qquad (3)$$

where L is the inductance, R the the series load resistance, and KL the mutual inductance. If we define $Q = \omega L/R$ and $I_2 = I_1 \exp[i(\pi/2)]$, then

$$V_1 = j\omega L I_1 + R \cdot (1 - KQ) I_1 \ , \qquad (4)$$
$$V_2 = j\omega L I_2 + R \cdot (1 + KQ) I_2 \ . \qquad (5)$$

This leads to a condition of negative power if KQ > 1. In an n-strap array, the net effect of the mutual coupling (for equal mutual coupling coefficients between adjacent straps and near-zero coupling for straps separated by one or more cavities) is that the middle straps' negative coupling on one side is cancelled by the positive coupling on the other side. The straps on the outside ends behave almost like those in the two-strap illustration above.

The DIII-D circuit parameters have been calculated and measured on the mock-ups. With no septum, the coupling coefficient K can be as high as 12%; coupling can be as low as 1% with solid septa. The resistive loading to the plasma increases with mutual coupling, but not dramatically enough to overwhelm the critical coupling. For the configuration chosen for DIII-D, the strap characteristic impedance was measured to be 35 Ω with a phase velocity of 53%, and the mutual coupling was ≈4.5%. At 6 Ω/m, this makes KQ ≈ 0.5. Since the loading is uncertain, the circuit needs to be able to cope with the negative power. Figure 4 shows the circuit for DIII-D. The outside antennas are paired so that the nearly negative power leg can resonate with the positive power leg and maintain phase. The paired circuit was tested on the mock-up, and KQ ≈ 11 (no load) was achieved with the antenna current ratio within 3% of unity and with phase within 2° of 90°.

Figure 5 shows the resultant phase and current on the straps for the matching configuration above with a load of 2.5 Ω/m (KQ = 1.2). During a plasma shot, the load is likely to change and the antenna can become slightly mismatched. The DIII-D antenna circuit was optimized to unbalance the amplitude (as opposed to the phase) for mismatching and tuning variations. This was done because a change in phase results in a shift in the spectrum, while a change in amplitude slightly reduces the current drive peak but does not change the dominant $n_{||}$. Figure 6 show how variations in loading affect the spectrum. A 50% change in loading reduces the current drive directivity from 85% to 73% and is considered to be sufficiently stable. The power that remains in the higher wave numbers is essentially the same.

DESIGN CONSIDERATIONS FOR ITER

The extension to ITER is based on the technology developed for DIII-D; however, the high-field tokamak with greater power and density changes the scenario. The frequency range has not been settled and extends from 20 MHz (favoring TTMP) to 120 MHz (favoring Landau damping). These choices open up three options: for the 20- to 65-MHz range, an in-blanket loop or a in-port loop array, and for 120 MHz, an in-port waveguide array. Figure 7 shows a plan view of the in-blanket array, which consists of 30 to 60 shorted straps placed about the tokamak off axis. The power would be 2.5 to 5 MW per antenna, depending on the number of powered straps. Figure 8 shows a plan view of the in-port folded waveguide array, which is a 4 × 12 array. This array is inserted into two ports and is exactly the analog of the in-port loop arrangement. All three configurations appear feasible, though each arrangement has its strong points.

The array of loops will have at least 12 loops in the array (toroidally). Directionality of either the in-port or the in-blanket arrangement is very high (>97%) and is not expected to be a problem. The periodicity of the array factor probably implies that some slotting will be needed to avoid undesired high-wave-number power.

The circuit problem for ITER is simpler than that for the DIII-D arrangement. Because the rf power per loop is comparable to a single transmitter module size, each antenna will have its own transmitter. The ability to couple the outside straps or waveguides is likely to be eliminated without a circulating power system. However, since the line-average density is almost 1×10^{14} cm^{-3}, the loading is expected to be considerably higher. KQ is expected to be no greater than 0.1, and thus straps could be run with a balanced power. This would result in imbalances of current at the ends of less than 5%, which has no significant impact on the spectrum.

The choice among the three configurations will have to be based on information that is not yet available. The folded waveguide looks especially attractive for a range of 60 to 120 MHz. It features no exposed ceramics and has the strongest structure of the three arrangements. Recent tests on the RF Test Facility at ORNL have shown that the

unloaded waveguide (with a $Q \approx 1600$) can achieve 200-kW operation, which is equivalent to 4 MW per loop antenna with plasma. The low internal fields facilitate this high power. The choice for the waveguide will hinge on whether its superior theoretical current drive efficiency at high frequency is offset by alpha particle absorption.

The in-blanket 20- to 65-MHz array is attractive because it uses no port space, but this approach complicates maintenance because the antenna cannot easily be removed from the tokamak. The power density can be a factor of two lower than in-port designs, but loading on the in-blanket design is compromised by the short radiating strap and possibly by off-axis launching.

The in-port 20- to 65-MHz loop arrangement requires two ports and seems to be attractive for the low frequency range. The midplane coupling and the more effective use of the radiating elements should give the best coupling and facilitate higher power density (1 kW/cm^2). Although it would be desirable to use space between ports for the array, this is not necessary for good spectral content. Thus, this antenna has the most maintainable configuration.

CONCLUSION

The prospects for FWCD are very encouraging. The POP experiment for DIII-D requires that phasing and spectral balances be made. However, the design laid out is *directional, and the circuit could handle high KQ. The* extension to ITER requires that the same trade-offs be made in concert with the reactor environment. If efficient FWCD can be demonstrated, it would make rf a very attractive option for ITER that could replace the more expensive heating and current drive systems that are now being proposed.

REFERENCES

[1] D. W. Swain et al., "Fast-Wave Ion Cyclotron Current Drive for ITER and Prospects for Near-Term Proof of Principles," to be published in the Proceedings of the 10th European Physical Society Meeting, Venice, 1989.

[2] D. Ehst, "RF Power Applications for ITER," in *Proc. RF Power in Plasmas (Eighth Topical Conference)*, Irvine, California, 1989, p. 393.

[3] D. B. Batchelor et al., "Fast-Wave Current Drive Modeling for ITER and Prospects for a Near Term Proof of Principle Experiment," in *Proc. RF Power in Plasmas (Eighth Topical Conference)*, Irvine, California, 1989, p. 219.

[4] T. K. Mau, "Studies of Fast Wave Current Drive in Reactors," *Bull. Am. Phys.*, vol. 33, No. 9, p. 1900, 1988.

[5] F. W. Baity et al., "Spectral Shaping and Phase Control of a Fast-Wave Current Drive Antenna Array," in *Proc. RF Power in Plasmas (Eighth Topical Conference)*, Irvine, California, 1989, p. 214.

[6] M. J. Mayberry et al., "60 MHz Fast-Wave Current Drive Experiment for DIII-D," in *Proc. RF Power in Plasmas (Eighth Topical Conference)*, Irvine, California, 1989, p. 298.

Figure Captions

Fig. 1. The 2-MW, four-strap FWCD for DIII-D. The Faraday shield elements are not shown.

Fig. 2. Comparison of power spectra for the four-strap array with solid side walls and with slotted sidewalls.

Fig. 3. Array factors for a 4-element array and a 12-element array with constant displacement and 90° phase difference between adjacent straps.

Fig. 4. Matching arrangement for the DIII-D experiment.

Fig. 5. Current amplitude and phase changes as a result of load changes. The antenna is tuned to 2.5 Ω/m in this example.

Fig. 6. Changes in the power spectrum resulting from load changes with the antenna matched to 2.5 Ω/m. The spectra that result from a load shift to 1.25 Ω/m and 3.75 Ω/m are shown.

Fig. 7. In-blanket loop FWCD array for ITER.

Fig. 8. In-port FWCD folded waveguide array for ITER.

FAST WAVE CURRENT DRIVE ANTENNA FOR DIII-D

ORNL-DWG 89-2866 FED

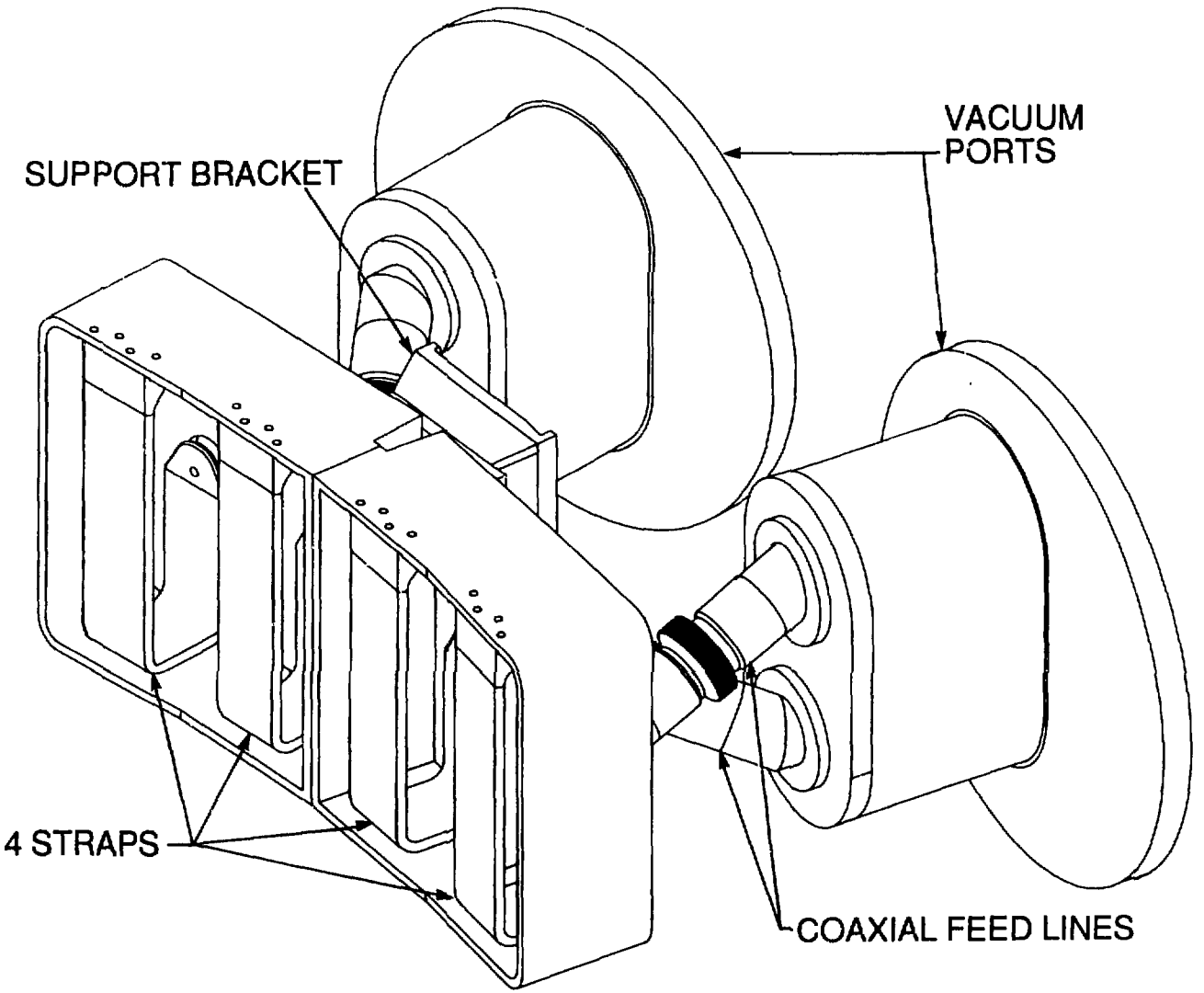

POWER SPECTRUM WITH AND WITHOUT SEPTA

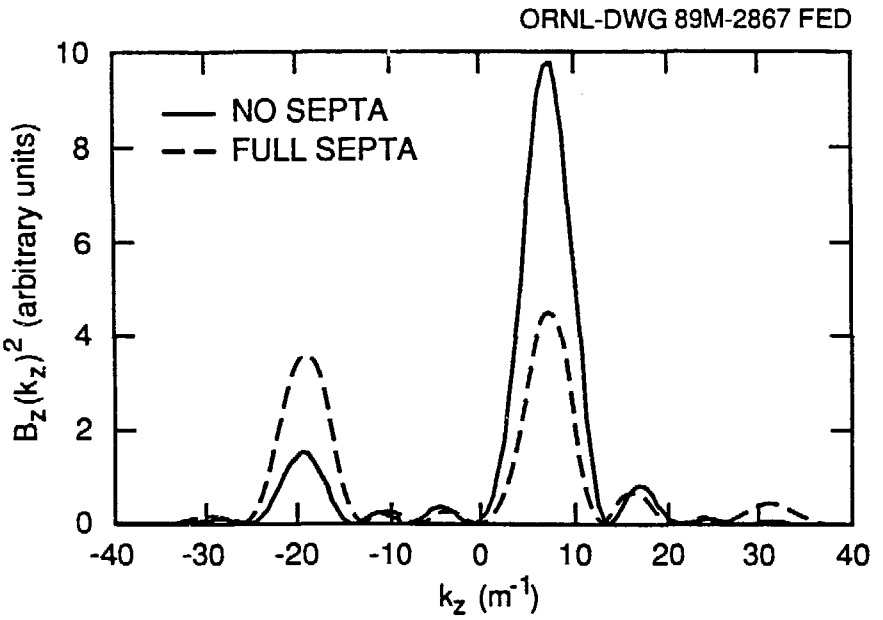

AMPLITUDE OF ARRAY FACTORS (4 AND 12 ELEMENT ARRAYS)

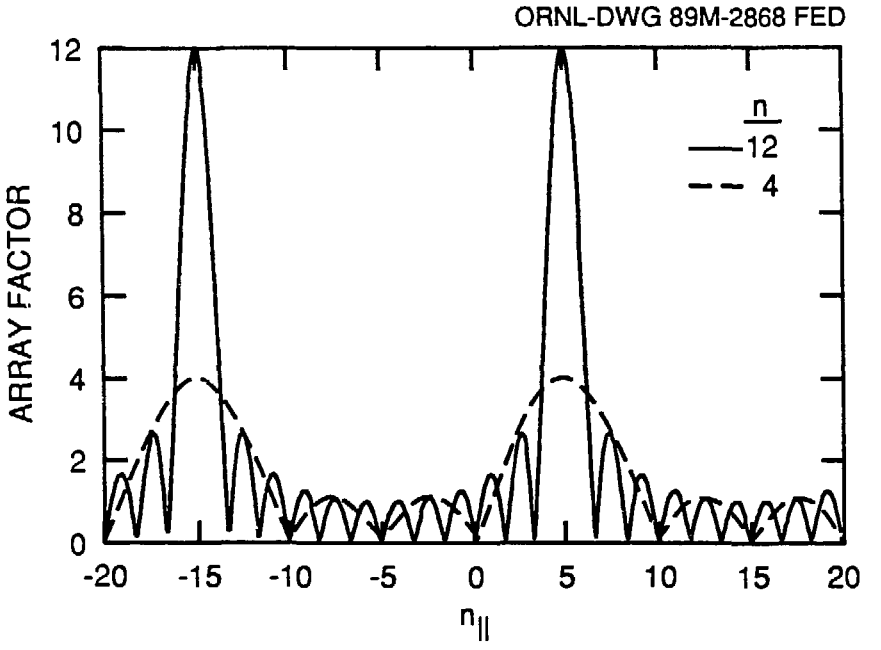

FEED CIRCUIT SCHEMATIC FOR DIII-D CURRENT DRIVE ANTENNA

ORNL-DWG 89M-2869 FED

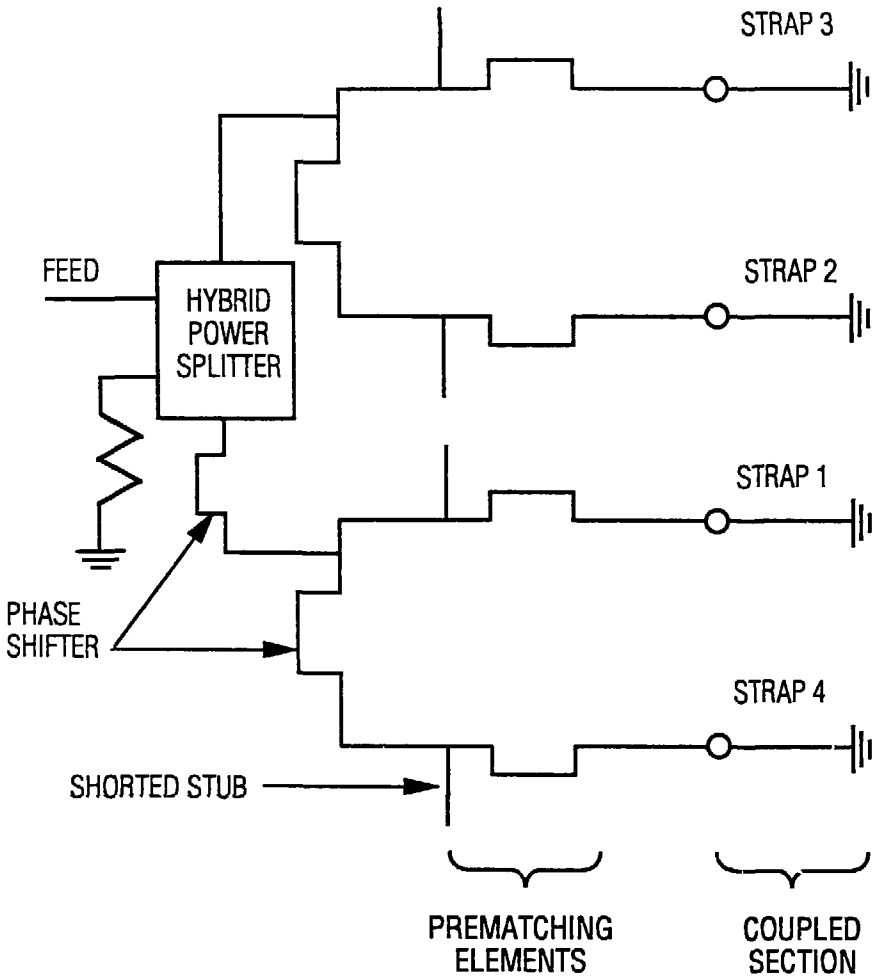

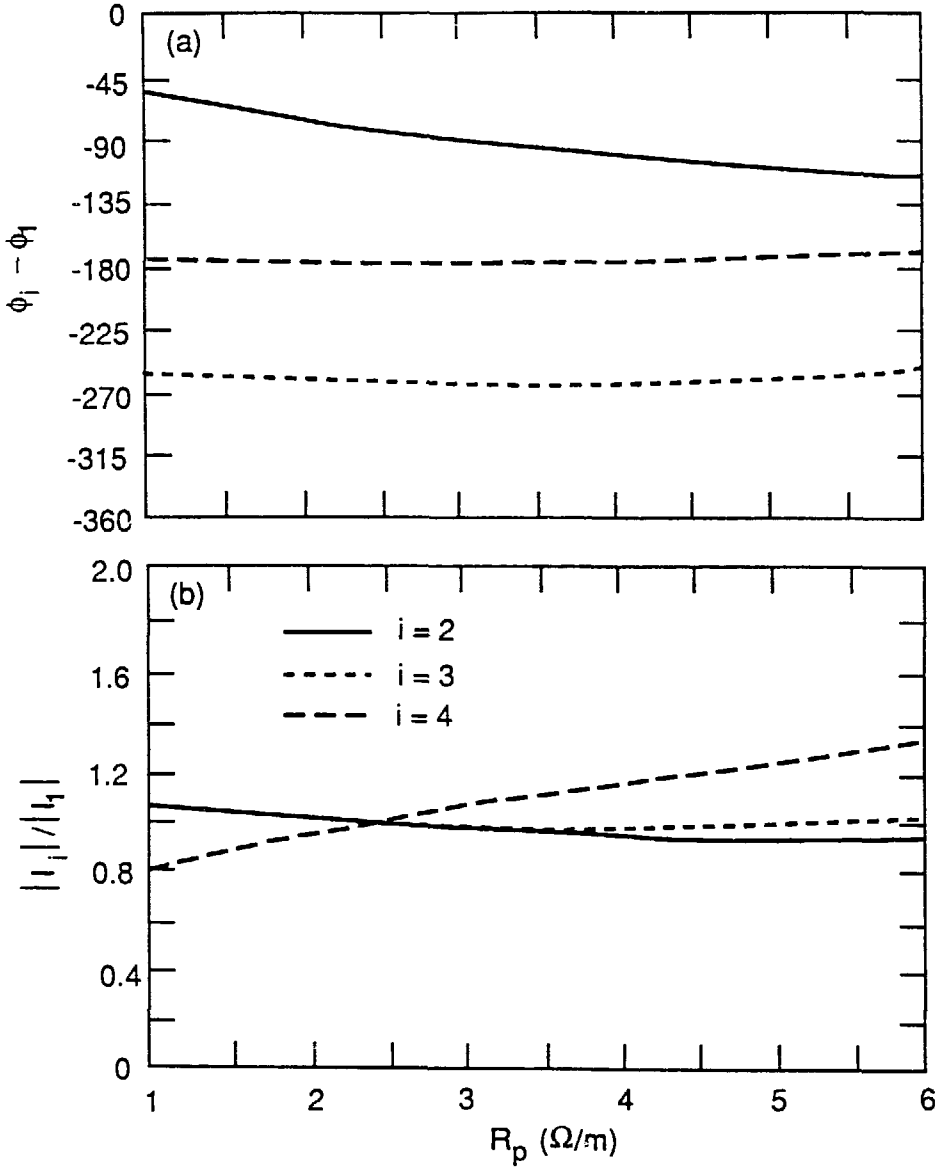
(a)
0
-45
-90
-135
-180
-225
-270
-315
-360
$\phi_i - \phi_1$
(b)
i = 2
i = 3
i = 4
2.0
1.6
1.2
0.8
0.4
0
$|I_i|/|I_1|$
1
2
3
4
5
6
R_p (Ω/m)

MODIFICATION OF THE SPECTRUM DUE TO TUNING MISMATCHES

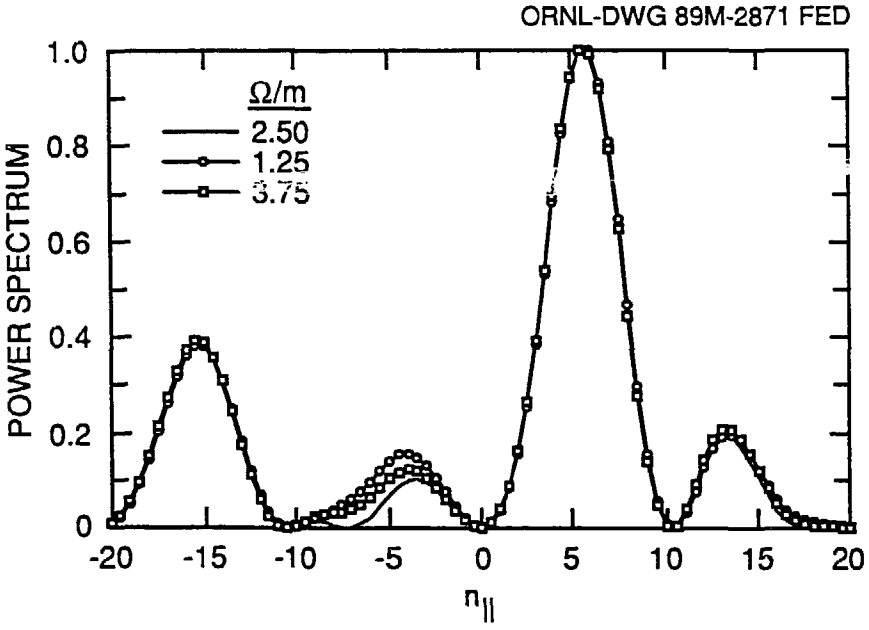

IN-BLANKET ARRAY

ORNL-DWG 89-2872 FED

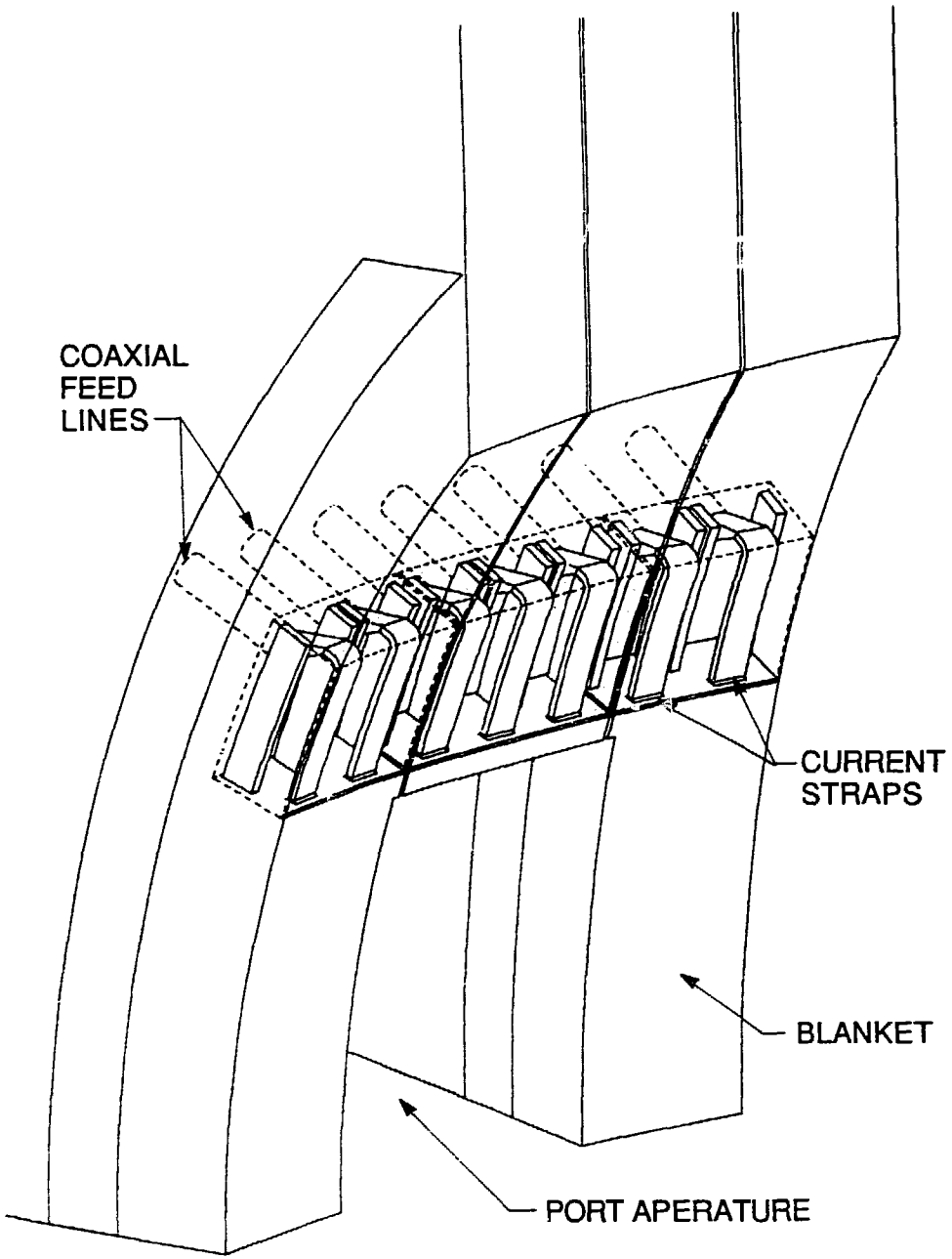

FOLDED WAVEGUIDE LAUNCHER FOR FAST WAVE CURRENT DRIVE IN ITER

ORNL-DWG 89-2873 FED